lengths are indicated by horizontal bars. Within these experimental uncertainties, a correlation of the form

$$\lambda_{max}\ (nm) = (4.83 \pm 0.03)r^6\ (Å^6) + (187 \pm 2)$$

seems to hold (correlation coefficient = 0.824). In Figure 2 are plotted the data points not only for $[Co(diamine)_3]^{3+}$ but also for complexes containing secondary (entries 8–11, 17, and 18) and tertiary (entry 12) amines. Thus, it is very satisfactory to find the data point for $[Co(L)(en)]^{3+}$ (an open circle in Figure 2) directly on the suggested correlation region.

In summary, the following conclusions may be drawn. Since an N–Co–N angle as small as 76.4° has not been reported to date, the effect of the chelate bite angle on the position of the absorption maximum cannot be properly assessed. Also, the problem of unusually high absorption intensity is not resolved. Figure 2 seems, however, to suggest strongly that the main cause for the red shift of the present complex lies in the relatively long Co–N bond lengths.

Acknowledgment. The authors are grateful to Dr. Yoshimasa Fukazawa for many helpful suggestions.

Registry No. en, 107-15-3; $[Co(L)(en)](ClO_4)_3$, 89907-10-8; Λ-$[Co(L)(en)](ClO_4)_3$, 91199-93-8; $[Co(sen)]Cl_3$, 82796-46-1; *trans*-$[CoCl_2(py)_4]Cl$, 27883-34-7; Co, 7440-48-4; 1,1,1-tris(hydroxymethyl)ethane, 77-85-0.

Supplementary Material Available: Listings of observed and calculated structure factor amplitudes, final atomic coordinates for hydrogen atoms with isotropic thermal parameters (Table II), final anisotropic thermal parameters for non-hydrogen atoms (Table III), and important hydrogen bond distances (Table VI) (23 pages). Ordering information is given on any current masthead page.

Contribution from the Chemistry Department, Wayne State University, Detroit, Michigan 48202

Trinuclear Complexes of 1,3,5,7-Tetraketonates. Synthesis, Molecular Structure, Absorption Spectra, and Electrochemistry of Several Bis[1,7-diphenyl-1,3,5,7-heptanetetronato(3–)]bis[dioxouranium(VI)]metal(II)–4-Pyridine Complexes

R. L. LINTVEDT,* B. A. SCHOENFELNER, C. CECCARELLI, and M. D. GLICK

Received May 17, 1983

Several heterotrinuclear complexes have been prepared with the ligand 1,7-diphenyl-1,3,5,7-heptanetetrone. Two UO_2^{2+} ions occupy the terminal coordination positions in the molecules, and a divalent transition-metal ion occupies the central position. Crystallization from pyridine yields compounds abbreviated as $(UO_2)_2M(DBAA)_2(py)_4 \cdot 2py$, where M(II) = Zn, Cu, Ni, Co, Fe, Mn. The X-ray crystal structures of the compounds where M is Ni(II), Co(II), Fe(II), and Mn(II) are reported. The structures are isomorphous. All are in the monoclinic space group $P2_1/c$. There are two molecules in the unit cell of each. The lattice constants with esd's, arranged in the sequence a, b, c (all in Å), β (in degrees), and V (in Å^3), are as follows: 13.436 (3), 24.011 (6), 10.566 (2), 108.12 (1), 3236 (1), for M = Ni; 13.45 (2), 23.93 (3), 10.62 (1), 108.3 (1), 3245 (8), for M = Co; 13.475 (2), 23.778 (3), 10.718 (1), 108.85(1), 3250 (1), for M = Fe; 13.473 (6), 23.507 (12), 10.834 (4), 109.08 (3), 3243 (2), for M = Mn. Cyclic voltammetric studies show that the U(VI) ions undergo quasi-reversible one-electron reductions in dimethylformamide with a platinum-disk electrode. The two ions yield two well-formed CV waves in the scan rate range of 0.020–2.000 V/s with a separation of 0.17–0.26 V. The separation is dependent upon the identity of the intervening transition metal. Differential pulse polarography was also employed to determine the peak separation values. The results were used to calculate conproportionality constants for the series. The values vary from about 2×10^3 to 2×10^4 in regular fashion going from Fe to Zn. The UV–visible spectral properties are also discussed.

Introduction

The β-polyketones are an homologous series potentially capable of forming a homologous series of polynuclear metal complexes. As such, they furnish an unusual opportunity to investigate the effect on chemical and physical properties of systematically increasing the number of interacting metal ions per molecule. The simplest members of the series, the bis(1,3-diketonato)metal complexes, have been extremely well studied throughout the history of modern coordination chemistry. The second members, the bis(1,3,5-triketonato)dimetal complexes, however, have been known only for about the past 15 years.[1] The third members, the bis(1,3,5,7-tetraketonato)trimetal complexes, are virtually unstudied. Two initial communications from our laboratory[2,3] are the only reports of trinuclear complexes of this interesting class of ligands. The work reported herein represents the first structural characterization of trinuclear 1,3,5,7-tetraketonates and establishes their ability to form trinuclear molecular complexes in a manner analogous to that for the mono- and dinuclear complexes of the 1,3-di- and 1,3,5-triketonates.

Table I. Comparison between the Calculated and Observed Elemental Analyses for $[(UO_2)_2M(DBAA)_2(py)_4] \cdot 2py$, $C_{68}H_{56}O_{12}N_6U_2M$

element		M = Mn	Fe	Co	Ni	Cu	Zn
C	calcd	48.61	48.58	48.49	48.51	48.36	48.31
	obsd	48.56	48.50	48.23	48.35	47.80	48.66
H	calcd	3.36	3.36	3.35	3.35	3.34	3.34
	obsd	3.42	3.53	3.45	3.39	3.37	3.53
N	calcd	5.00	5.00	4.99	4.99	4.98	4.97
	obsd	4.93	5.03	4.98	4.97	4.77	5.14
U	calcd	28.33	28.32	28.27	28.27	28.19	28.16
	obsd	28.40	28.06	27.30	28.56	28.50	27.85
M	calcd	3.27	3.32	3.50	3.49	3.76	3.87
	obsd	3.13	3.13	3.48	3.52	3.80	3.86

(1) Some of the earliest studies are: Baker, D.; Dudley, C. W.; Oldham, C. *J. Chem. Soc. A* **1970**, 2605. Murtha, D. P.; Lintvedt, R. L. *Inorg. Chem.* **1970**, *9*, 1532. Sagard, F.; Kobayashi, H.; Ueno, K. *Bull. Chem. Soc. Jpn.* **1968**, *41*, 266; **1972**, *45*, 794.
(2) Andrelczyk, B.; Lintvedt, R. L. *J. Am. Chem. Soc.* **1972**, *94*, 8633.
(3) Lintvedt, R. L.; Schoenfelner, B. A.; Ceccarelli, C.; Glick, M. D. *Inorg. Chem.* **1982**, *21*, 2113.

0020-1669/84/1323-2867$01.50/0

Experimental Section

Ligand Synthesis. The ligand, 1,7-diphenyl-1,3,5,7-heptanetetrone, H_3DBAA, was prepared according to methods developed by Harris and co-workers.[4]

Synthesis of the Complexes, $(UO_2)_2M(DBAA)_2(py)_4 \cdot 2py$. Dissolve 4.13 g (9.73 mmol) of $UO_2(CH_3COO)_2 \cdot 2H_2O$ and 4.86 mmol of the appropriate transition-metal acetate in 150 mL of boiling absolute CH_3OH. To this solution add 3.00 g (9.73 mmol) of H_3DBAA, boil for 5 min, and add 25 mL of $(C_2H_5)_3N$. Boil for 5 min more and filter while still hot. Wash the dark-colored solid with absolute CH_3OH and air-dry. Dissolve the crude product in pyridine and reduce the volume with a slow stream of N_2. Crystals form immediately. The yield was not maximized, but 2–3 g was obtained. The results of elemental analyses are presented in Table I.

Electrochemistry. Cyclic voltammetric, CV, procedures and apparatus have recently been described.[5] CV experiments made use of Pt-disk or hanging mercury drop electrodes. Differential pulse polarography, DPP, and reverse pulse polarography, RPP, were performed with an EG & G PAR Model 174A polarographic analyzer and a Model 303 SMDE using a LiCl/AgCl reference electrode.

Spectral Measurements. The UV–visible spectra were obtained in ethanol on a Cary 17 spectrophotometer.

Crystallography and Structure Determination. Table II provides the relevant information regarding the X-ray diffraction experiments that were undertaken. Atomic coordinates can be found in Tables III–VI. Bond distances and angles in the coordination spheres of the metals are in Table VII. Tables of bond distances and angles for the ligand atoms, hydrogen atom parameters, thermal parameters of the non-hydrogen atoms, and observed and calculated structure factors have been deposited as supplementary material.

Results

1. Structure of $(UO_2)_2M(DBAA)_2(py)_4$. The complexes $(UO_2)_2M(DBAA)_2(py)_4$, where M = Ni(II), Co(II), Fe(II), Mn(II) and $DBAA^{3-}$ is the trianion of 1,7-diphenyl-1,3,5,7-heptanetetrone, form a series that yield isomorphous crystals from pyridine. The uranyl ions occupy the terminal coordination positions with four ketonate oxygens and one pyridine nitrogen comprising the five equatorial donor atoms in a distorted-pentagonal-bipyramidal coordination sphere geometry. The bond distances and angles around the uranium atoms in each of the four molecules are virtually identical. The divalent transition-metal ion occupies the central coordination position and is bound to four ketonate oxygens, which all act as bridging atoms between the transition metal and uranium atoms. In addition, pyridine nitrogen atoms occupy the fifth and sixth coordination positions above and below the plane of the tetraketonates. The M–O bond lengths are quite normal for high-spin d^8, d^7, d^6, and d^5 metal ions of the first transition series with the expected orderly increase from Ni(II) to Mn(II). The M–N axial bond distance also increase in the order Ni < Co < Fe < Mn, but at a greater rate. That is, the M–N bond distance increases in a monotonic fashion about 0.06 Å with an increase of 1 in the atomic number of M. The U–M distance is quite similar in all four compounds at about 3.520 (±0.001) Å. The O–M–O bond angles are quite similar, varying only from 92.6 to 94.1° for the "diketonate-type" intraligand angle and from 85.9 to 87.4° for the interligand angle in which both oxygens are bonded to the same uranium atom. These values are not at all unusual and indicate an absence of any important strain associated with the coordination of the central metal ion. Finally, the tetraketonate ligand atoms, excluding the phenyls, and the three metal atoms are essentially coplanar with no atom varying by more than about 0.478 Å from a "best plane" fit. An ORTEP drawing of one of the molecules is shown in Figure 1. A view of the molecule in the molecular plane with the atom-numbering scheme for the principal atoms in given in Figure 2.

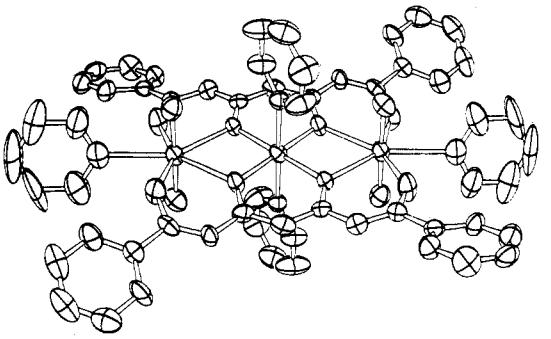

Figure 1. ORTEP drawing of $(UO_2)_2Fe(DBAA)_2(py)_4$. Thermal ellipsoids are at 50% probability.

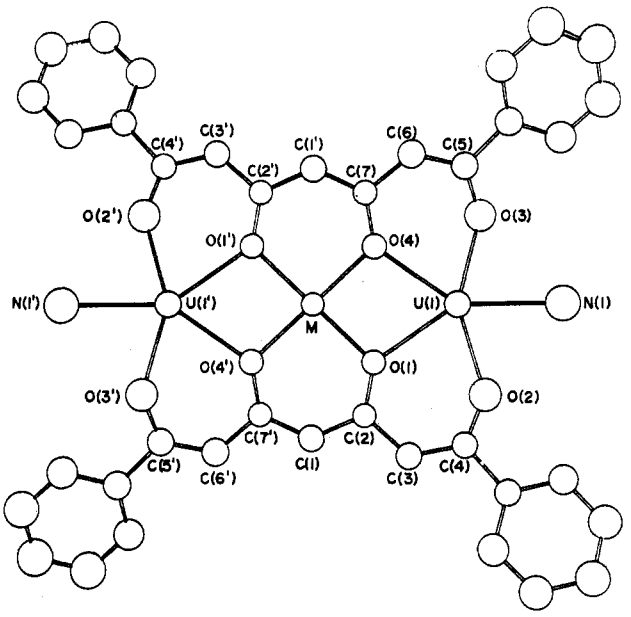

Figure 2. Simplified representation of the in-plane ligand and metal atoms.

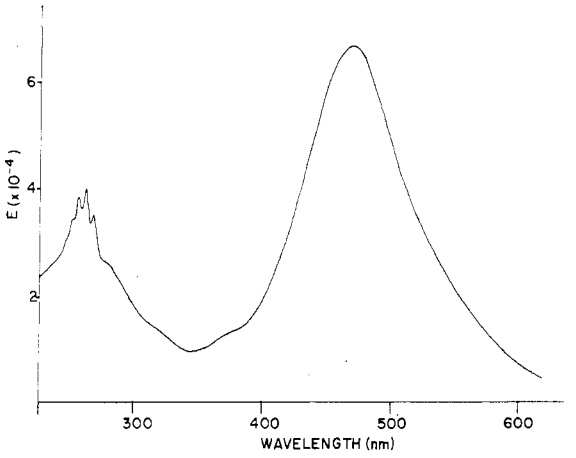

Figure 3. UV–visible spectrum of $(UO_2)_2Ni(DBAA)_2(py)_4$ in ethanol, 2.70×10^{-5} M.

2. Absorption Spectra. These trinuclear complexes all exhibit two very intense bands in the UV–visible region of the spectrum. A typical spectrum is shown in Figure 3. The low-energy band, whose maximum occurs between 466 and 472 nm, has an extinction coefficient between about 2×10^4 and 9×10^4. The energy of the band maximum does not appear to be much affected by changes in the transition-metal ion. However, the intensities of the band maxima decrease regulary from M = Zn ($E_{max} = 9.5 \times 10^5$ L/(mol cm)) to M

(4) Sandifer, R. M.; Bhattacharya, A. K. Harris, T. M., *J. Org. Chem.* **1981**, *46*, 2260.
(5) Lintvedt, R. L.; Kramer, L. S. *Inorg. Chem.* **1983**, *22*, 796.

Table II. X-ray Experimental Data for $[(UO_2)_2M(DBAA)_2(py)_4]\cdot 2py$

	M			
	Ni	Co	Fe	Mn
radiation used	Mo Kα	Mo Kα	Mo Kα	Mo Kα
space group	$P2_1/c$	$P2_1/c$	$P2_1/c$	$P2_1/c$
max cryst dimens, mm	0.67 × 0.21 × 0.19	0.67 × 0.26 × 0.16	0.28 × 0.25 × 0.04	0.38 × 0.24 × 0.19
ρ_{exptl}, g/cm^3	1.733	1.729	1.724	1.727
lattice constants				
a, Å	13.436 (3)	13.45 (2)	13.475 (2)	13.473 (6)
b, Å	24.011 (6)	23.93 (3)	23.778 (3)	23.507 (12)
c, Å	10.556 (2)	10.62 (1)	10.718 (1)	10.834 (4)
β, deg	108.12 (1)	108.3 (1)	108.85 (1)	109.08 (3)
V, Å^3	3236 (1)	3245 (8)	3250 (1)	3243 (2)
data collection				
type of scan	$\theta/2\theta$	$\theta/2\theta$	$\theta/2\theta$	$\theta/2\theta$
scan range, deg	$K\alpha_1 - 1$ to $K\alpha_2 + 1$	$K\alpha_1 - 1$ to $K\alpha_2 + 1$	$K\alpha_1 - 1$ to $K\alpha_2 + 1$	$K\alpha_1 - 1$ to $K\alpha_2 + 1$
scan rate, deg/min	fixed, 2	fixed, 2	fixed, 2	variable, 2-5
bkgd:scan time	0.20	0.20	0.50	0.50
collection region	$\pm h+k+l$	$\pm h+k+l$	$\pm h+k\pm l$	$\pm h+k+l$
2θ limits, deg	$2 \leq 2\theta \leq 45$	$2 \leq 2\theta \leq 45$	$2 \leq 2\theta \leq 45$	$4 \leq 2\theta \leq 45$
reflcns measd[a]	4865	4947	4835	4946
std reflcns	$(\bar{4}04)$, $(\bar{4}0\bar{2})$, (080)	$(\bar{4}04)$, $(\bar{4}0\bar{2})$, (080)	$(40\bar{4})$, (402), (080)	(004), $(60\bar{2})$, (080)
how of 10 measd	every 97 data	every 97 data	every 97 data	every 97 data
decay	negligible	negligible	negligible	negligible
data reduction				
corrections applied	Lp	Lp	Lp	Lp
$\sigma(F_o^2)$[b]	$(\sigma_c^2 + 0.05F_o^2)^{1/2}$	$(\sigma_c^2 + 0.05F_o^2)^{1/2}$	$(\sigma_c^2 + 0.05F_o^2)^{1/2}$	$(\sigma_c^2 + 0.05F_o^2)^{1/2}$
obsd reflcn	$F_o^2 > 3\sigma(F_o^2)$	$F_o^2 \geq 3\sigma(F_o^2)$	$F_o^2 \geq 3\sigma(F_o^2)$	$F_o^2 \geq 3\sigma(F_o^2)$
unique obsd reflcns	2961	2568	2644	2899
absorption				
μ, cm^{-1}	50.85	50.72	49.96	50.75
correction method	ref 17, 18	ref 17, 18	ref 17, 18	ref 17, 18
abs factors	2.301-2.675	2.168-3.442	1.223-2.829	2.107-2.593
soln method	F^2 Patterson, F_o $F_o - F_c$ synthesis	replacement of Ni by Co	replacement of Ni by Fe	replacement of Ni by Mn
H atoms				
how located	calcd	calcd	calcd	calcd
bond dist, Å	0.95	0.95	0.95	0.95
spatial arrangement	sp^2	sp^2	sp^2	sp^2
temp factor	$B_H = 1.10B_C$	$B_H = 1.10B_C$	$B_H = 1.10B_C$	$B_H = 1.10B_C$
refinement				
method	full-matrix least squares	full-matrix least squares	full-matrix least squares	full-matrix least squares
wt	$w = [1/\sigma(F_o)]^2$	$w = [1/\sigma(F_o)]^2$	$w = [1/\sigma(F_o)]^2$	$w = [1/\sigma(F_o)]^2$
quantity minimized	$\Sigma w(\lvert F_o\rvert - \lvert F_c\rvert)^2$	$\Sigma w(\lvert F_o\rvert - \lvert F_c\rvert)^2$	$\Sigma w(\lvert F_o\rvert - \lvert F_c\rvert)^2$	$\Sigma w(\lvert F_o\rvert - \lvert F_c\rvert)^2$
non-H atoms	anisotropic	anisotropic	anisotropic	anisotropic
solvent atoms	isotropic	isotropic	isotropic	isotropic
H atoms	fixed	fixed	fixed	fixed
variable parameters	373	373	373	373
R_1[c]	0.031	0.039	0.035	0.040
R_2[d]	0.038	0.048	0.040	0.046
S[e]	1.114	1.333	1.063	1.337
residual electron density, $\Delta\rho_{max}$, e/Å^3	1.01	1.08	0.81	1.87
scattering factors[f]	ref 19-21	ref 19-21	ref 19-21	ref 19-21

[a] This number includes standards and ψ-scan data. The latter were used to check the absorption correction. [b] σ_c is from counting statistics. [c] $R_1 = \Sigma\lvert\lvert F_o\rvert - \lvert F_c\rvert\rvert/\Sigma\lvert F_o\rvert$. [d] $R_2 = [\Sigma w(\lvert F_o\rvert - \lvert F_c\rvert)^2/\Sigma w\lvert F_o\rvert^2]^{1/2}$. [e] $S = [w(\lvert F_o\rvert - \lvert F_c\rvert)^2/(NO - NV)]^{1/2}$, where NO is the number of observations and NV is the number of variable parameters. [f] Neutral-atom scattering factors were used. The anomalous components $\Delta f'$ and $\Delta f''$ were included for U, Ni, Co, Fe, and Mn.

= Mn (E_{max} = 2.3 × 10^4 L/(mol cm)). The high-energy band is centered at about 260 nm with an extinction coefficient of about 4 × 10^4 L/(mol cm). Four or five well-resolved peaks with separations of about 6–10 nm are observed for each compound. The general characteristics of this high-energy band including wavelength and extinction coefficients are reasonably independent of changes in the transition-metal ions. The observation of any d–d bands is presumably obscured by the intense, broad absorption at 470 nm. No evidence for d–d absorption could be found.

3. Electrochemical Properties. The cyclic voltammograms (CV) of all the complexes in DMF at a Pt-disk electrode exhibited two very nearly reversible waves at about −1.1 and −1.3 V vs. SSCE. Figure 4 is the CV of the zinc complex in which only the U(VI)'s are reducible in the region 0 to −1.7 V. Under these conditions the first wave has a peak separation,

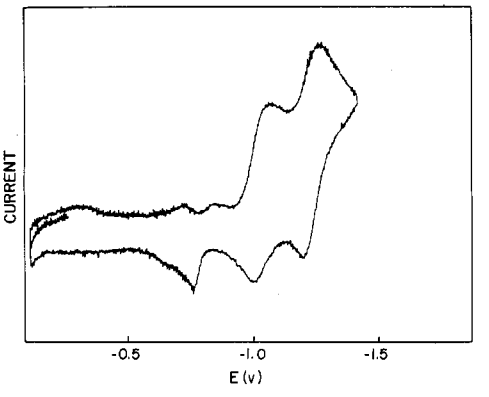

Figure 4. Cyclic voltammogram of 0.0008 M $(UO_2)_2Zn(DBAA)_2(py)_4$ in DMF with 0.100 M TEAP at a HMDE. Scan rate is 200 mV/s.

Table III. Atomic Coordinates for $[(UO_2)_2Ni(DBAA)_2(py)_4]\cdot py$[a]

atom	x	y	z
U(1)	0.09668 (2)	0.11515 (1)	−0.13152 (3)
Ni(1)	0	0	0
O(1)	0.2665 (4)	0.1217 (3)	−0.0104 (7)
O(2)	0.1418 (4)	0.0349 (2)	0.0193 (5)
O(3)	0.0606 (4)	−0.0627 (2)	0.1299 (5)
O(4)	0.0398 (4)	−0.1484 (3)	0.2974 (6)
O(5)	0.0662 (4)	0.1595 (3)	−0.0165 (6)
O(6)	0.1298 (5)	0.0738 (3)	−0.2504 (6)
N(1)	0.1685 (6)	0.2024 (5)	−0.2170 (9)
N(2)	−0.0083 (5)	0.0501 (3)	0.1681 (6)
C(1)	0.3426 (6)	0.0861 (4)	0.0360 (8)
C(2)	0.3278 (6)	0.0348 (4)	0.0794 (8)
C(3)	0.2298 (6)	0.0103 (3)	0.0810 (7)
C(4)	0.2373 (6)	−0.0375 (4)	0.1553 (8)
C(5)	0.1601 (6)	−0.0695 (3)	0.1865 (7)
C(6)	0.1989 (6)	−0.1107 (4)	0.2884 (8)
C(7)	0.1403 (6)	−0.1453 (3)	0.3411 (8)
C(8)	0.1906 (6)	−0.1830 (3)	0.4574 (8)
C(9)	0.1331 (7)	−0.2275 (4)	0.4818 (9)
C(10)	0.1753 (8)	−0.2613 (4)	0.5915 (10)
C(11)	0.2735 (9)	−0.2515 (4)	0.6766 (10)
C(12)	0.3320 (7)	−0.2076 (5)	0.6518 (9)
C(13)	0.2916 (7)	−0.1736 (4)	0.5432 (9)
C(14)	0.4492 (6)	0.1080 (4)	0.0437 (8)
C(15)	0.4580 (7)	0.1616 (4)	0.0013 (9)
C(16)	0.5525 (8)	0.1826 (5)	0.0007 (11)
C(17)	0.6399 (9)	0.1497 (6)	0.0368 (11)
C(18)	0.6346 (7)	0.0961 (5)	0.0795 (12)
C(19)	0.5377 (7)	0.0753 (4)	0.0825 (10)
C(20)	0.2336 (11)	0.1962 (6)	−0.2857 (13)
C(21)	0.2901 (13)	0.2418 (10)	−0.3151 (18)
C(22)	0.2710 (16)	0.2941 (8)	−0.2701 (21)
C(23)	0.2052 (14)	0.2974 (7)	−0.2054 (20)
C(24)	0.1523 (11)	0.2522 (6)	−0.1790 (15)
C(25)	−0.0675 (7)	0.0953 (4)	0.1549 (9)
C(26)	−0.0726 (9)	0.1282 (4)	0.2605 (12)
C(27)	−0.0169 (9)	0.1111 (5)	0.3871 (11)
C(28)	0.0408 (11)	0.0656 (6)	0.4022 (11)
C(29)	0.0446 (9)	0.0370 (4)	0.2915 (10)
NP(1)	−0.5335 (14)	0.0964 (7)	−0.3205 (18)
CP(1)	−0.6108 (15)	0.0604 (8)	−0.3156 (19)
CP(2)	−0.6648 (17)	0.0297 (10)	−0.4252 (25)
CP(3)	−0.6359 (16)	0.0436 (9)	−0.5356 (20)
CP(4)	−0.5637 (18)	0.0820 (10)	−0.5441 (22)
CP(5)	−0.5098 (16)	0.1129 (8)	−0.4351 (21)

[a] The standard deviations in parentheses refer to the least significant digit.

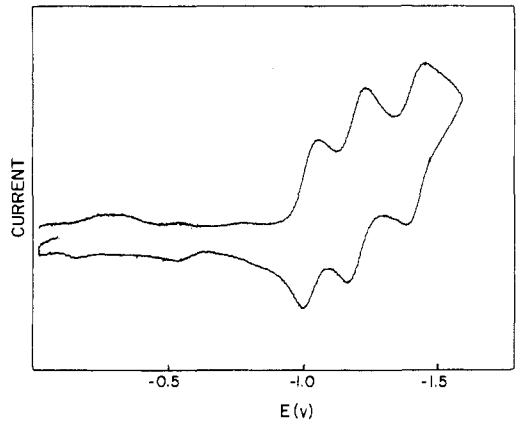

Figure 5. Cyclic voltammogram of 0.00073 M $(UO_2)_2Ni(DBAA)_2(py)_4$ in DMF with 0.100 M TEAP at a HMDE. Scan rate is 200 mV/s.

ΔE_p, of 62 mV and $E_{1/2}$ = −1.03 V vs. SSCE. The second wave has ΔE_p = 86 mV and $E_{1/2}$ = −1.28 V vs. SSCE. The spike at −0.47 V is due to the strong adsorption of one of the products. Figure 5 shows the CV of the Ni(II) complex, in which a third wave appears at about −1.6 V. This new wave

Table IV. Atomic Coordinates for $[(UO_2)_2Co(DBAA)_2(py)_4]\cdot 2py$[a]

atom	x	y	z
U(1)	0.09565 (4)	0.11559 (2)	−0.13121 (5)
Co(1)	0	0	0
O(1)	0.2664 (7)	0.1222 (4)	−0.0113 (10)
O(2)	0.1427 (7)	0.0349 (3)	0.0211 (8)
O(3)	0.0615 (7)	−0.0631 (3)	0.1313 (7)
O(4)	0.0415 (8)	−0.1481 (4)	0.2968 (9)
O(5)	0.0645 (7)	0.1596 (4)	−0.0161 (9)
O(6)	0.1263 (8)	0.0739 (4)	−0.2501 (9)
N(1)	0.1676 (11)	0.2026 (6)	−0.2153 (16)
N(2)	−0.0096 (8)	0.0510 (5)	0.1721 (10)
C(1)	0.3400 (10)	0.0874 (6)	0.0357 (12)
C(2)	0.3274 (10)	0.0352 (6)	0.0822 (13)
C(3)	0.2310 (10)	0.0103 (6)	0.0847 (12)
C(4)	0.2365 (10)	−0.0365 (6)	0.1569 (13)
C(5)	0.1624 (10)	−0.0702 (6)	0.1900 (12)
C(6)	0.1994 (10)	−0.1098 (6)	0.2922 (12)
C(7)	0.1426 (10)	−0.1456 (5)	0.3414 (12)
C(8)	0.1910 (11)	−0.1830 (6)	0.4559 (13)
C(9)	0.1358 (11)	−0.2273 (6)	0.4819 (13)
C(10)	0.1764 (13)	−0.2607 (6)	0.5900 (16)
C(11)	0.2754 (15)	−0.2508 (7)	0.6753 (16)
C(12)	0.3302 (12)	−0.2080 (7)	0.6549 (14)
C(13)	0.2927 (12)	−0.1735 (6)	0.5427 (15)
C(14)	0.4503 (10)	0.1068 (6)	0.0431 (13)
C(15)	0.4594 (12)	0.1617 (7)	0.0050 (13)
C(16)	0.5527 (14)	0.1833 (8)	−0.0012 (16)
C(17)	0.6408 (13)	0.1494 (9)	0.0370 (17)
C(18)	0.6349 (15)	0.0963 (8)	0.0775 (19)
C(19)	0.5346 (13)	0.0758 (7)	0.0793 (16)
C(20)	0.2319 (18)	0.1968 (9)	−0.2862 (21)
C(21)	0.2873 (23)	0.2432 (17)	−0.3135 (32)
C(22)	0.2719 (31)	0.2945 (16)	−0.2710 (44)
C(23)	0.2064 (25)	0.2986 (11)	−0.2034 (31)
C(24)	0.1543 (15)	0.2516 (10)	−0.1778 (22)
C(25)	−0.0649 (11)	0.0967 (7)	0.1578 (13)
C(26)	−0.0726 (15)	0.1293 (7)	0.2647 (20)
C(27)	−0.0186 (15)	0.1134 (8)	0.3878 (17)
C(28)	0.0393 (18)	0.0658 (8)	0.4040 (16)
C(29)	0.0411 (15)	0.0382 (7)	0.2952 (15)
NP(1)	−0.5295 (26)	0.0977 (12)	−0.3209 (31)
CP(1)	−0.6085 (25)	0.0626 (13)	−0.3145 (29)
CP(2)	−0.6624 (25)	0.0306 (13)	−0.4133 (35)
CP(3)	−0.6356 (25)	0.0403 (13)	−0.5312 (31)
CP(4)	−0.5761 (26)	0.0807 (14)	−0.5507 (30)
CP(5)	−0.5100 (26)	0.1133 (13)	−0.4439 (35)

[a] The standard deviations in parentheses refer to the least significant digit.

is undoubtedly due to the Ni(II) ⇌ Ni(I) electron-transfer process. Pertinent information about these waves up to scan rates of 2.00 V/s is given in Table VIII. Beyond 2.00 V/s the peak separations become too large to obtain meaningful data.

The CV's of $(UO_2)_2Cu(DBAA)_2(py)_4$ exhibit the usual two UO_2^{2+} waves preceded by a quasi-reversible Cu(II) ⇌ Cu(I) wave at about −0.5 V. The characteristics of this wave at scan rates from 0.020 to 5.00 V/s are given in Table IX. A hanging mercury drop electrode was used since the wave due to the Cu(II) ⇌ Cu(I) is much better behaved on Hg than on Pt. The compounds in which M = Co(II), Fe(II), Mn(II) exhibit no wave due to the transition-metal ion in the 0 to −1.7 V region in DMF with 0.1 M TEAP. Sweeps in the positive direction for compounds in which M = Mn(II), Co(II), Fe(II), Cu(II) show irreversible oxidations at peak potentials of +0.59, +0.61, +0.37, and +0.76 V vs. SSCE, respectively.

Differential pulse polarograms (DPP) on the compounds where M = Fe, Co, Ni, Cu, Zn were obtained to substantiate the one-electron nature of the uranium CV waves. In the limiting case, when the modulation amplitude is small, n may be determined from the peak half-width[6] by

$$W_{1/2} = 3.52RT/nF$$

Table V. Atomic Coordinates for $[(UO_2)_2Fe(DBAA)_2(py)_4]\cdot 2py$[a]

atom	x	y	z
U(1)	0.09486 (3)	0.11570 (2)	−0.13083 (4)
Fe(1)	0	0	0
O(1)	0.2661 (6)	0.1216 (4)	−0.0126 (8)
O(2)	0.1442 (5)	0.0346 (3)	0.0215 (6)
O(3)	0.0640 (5)	−0.0633 (3)	0.1321 (6)
O(4)	0.0444 (6)	−0.1501 (4)	0.2942 (7)
O(5)	0.0658 (6)	0.1609 (3)	−0.0168 (7)
O(6)	0.1256 (6)	0.0728 (4)	−0.2481 (7)
N(1)	0.1666 (8)	0.2021 (5)	−0.2167 (10)
N(2)	−0.0073 (7)	0.0534 (4)	0.1761 (8)
C(1)	0.3435 (9)	0.0868 (5)	0.0375 (10)
C(2)	0.3293 (8)	0.0357 (5)	0.0841 (10)
C(3)	0.2345 (8)	0.0110 (5)	0.0866 (9)
C(4)	0.2410 (8)	−0.0366 (5)	0.1636 (10)
C(5)	0.1653 (8)	−0.0702 (4)	0.1908 (9)
C(6)	0.2023 (8)	−0.1104 (5)	0.2939 (9)
C(7)	0.1436 (8)	−0.1461 (5)	0.3421 (9)
C(8)	0.1936 (9)	−0.1831 (5)	0.4593 (9)
C(9)	0.1354 (9)	−0.2285 (5)	0.4817 (10)
C(10)	0.1768 (11)	−0.2610 (5)	0.5921 (12)
C(11)	0.2765 (11)	−0.2508 (5)	0.6780 (11)
C(12)	0.3356 (10)	−0.2077 (6)	0.6559 (11)
C(13)	0.2931 (9)	−0.1744 (5)	0.5467 (10)
C(14)	0.4483 (8)	0.1090 (5)	0.0417 (9)
C(15)	0.4568 (9)	0.1647 (6)	0.0025 (11)
C(16)	0.5514 (13)	0.1853 (7)	−0.0009 (12)
C(17)	0.6384 (12)	0.1498 (9)	0.0332 (14)
C(18)	0.6330 (11)	0.0968 (7)	0.0760 (14)
C(19)	0.5375 (10)	0.0767 (6)	0.0812 (13)
C(20)	0.2309 (14)	0.1982 (7)	−0.2869 (14)
C(21)	0.2862 (17)	0.2449 (12)	−0.3110 (23)
C(22)	0.2678 (24)	0.2959 (12)	−0.2730 (28)
C(23)	0.2043 (21)	0.2994 (9)	−0.1987 (24)
C(24)	0.1516 (13)	0.2516 (7)	−0.1765 (16)
C(25)	−0.0663 (9)	0.0984 (6)	0.1601 (11)
C(26)	−0.0735 (12)	0.1304 (6)	0.2653 (14)
C(27)	−0.0181 (11)	0.1131 (7)	0.3907 (12)
C(28)	0.0417 (13)	0.0668 (7)	0.4075 (12)
C(29)	0.0434 (12)	0.0378 (6)	0.2983 (12)
NP(1)	−0.5404 (18)	0.0990 (9)	−0.3206 (20)
CP(1)	−0.6145 (20)	0.0587 (11)	−0.3172 (23)
CP(2)	−0.6642 (23)	0.0310 (12)	−0.4347 (31)
CP(3)	−0.6340 (21)	0.0450 (11)	−0.5372 (24)
CP(4)	−0.5610 (21)	0.0837 (11)	−0.5377 (24)
CP(5)	−0.5102 (19)	0.1151 (10)	−0.4318 (24)

[a] The standard deviations in parentheses refer to the least significant digit.

Table VI. Atomic Coordinates for $[(UO_2)_2Mn(DBAA)_2(py)_4]\cdot 2py$[a]

atom	x	y	z
U(1)	0.09564 (3)	0.11761 (2)	−0.13082 (4)
Mn(1)	0	0	0
O(1)	0.2689 (5)	0.1228 (3)	−0.0180 (8)
O(2)	0.1459 (5)	0.0362 (3)	0.0207 (6)
O(3)	0.0647 (5)	−0.0661 (3)	0.1322 (6)
O(4)	0.0443 (6)	−0.1541 (4)	0.2880 (7)
O(5)	0.0717 (6)	0.1617 (3)	−0.0155 (7)
O(6)	0.1211 (6)	0.0754 (3)	−0.2493 (7)
N(1)	0.1679 (8)	0.2063 (5)	−0.2137 (11)
N(2)	−0.0062 (7)	0.0545 (4)	0.1821 (9)
C(1)	0.3463 (8)	0.0877 (5)	0.0377 (10)
C(2)	0.3331 (8)	0.0369 (5)	0.0887 (10)
C(3)	0.2359 (8)	0.0128 (5)	0.0890 (10)
C(4)	0.2398 (8)	−0.0363 (5)	0.1654 (10)
C(5)	0.1650 (8)	−0.0707 (4)	0.1934 (9)
C(6)	0.2029 (8)	−0.1109 (5)	0.2954 (10)
C(7)	0.1444 (8)	−0.1485 (5)	0.3397 (9)
C(8)	0.1941 (8)	−0.1851 (5)	0.4593 (10)
C(9)	0.1371 (9)	−0.2300 (5)	0.4816 (10)
C(10)	0.1775 (11)	−0.2629 (5)	0.5911 (12)
C(11)	0.2762 (11)	−0.2510 (6)	0.6808 (12)
C(12)	0.3331 (10)	−0.2059 (6)	0.6553 (11)
C(13)	0.2915 (9)	−0.1736 (5)	0.5482 (10)
C(14)	0.4517 (8)	0.1088 (5)	0.0428 (10)
C(15)	0.4603 (9)	0.1637 (6)	0.0022 (12)
C(16)	0.5569 (11)	0.1843 (6)	0.0010 (13)
C(17)	0.6438 (10)	0.1490 (8)	0.0375 (14)
C(18)	0.6356 (10)	0.0965 (7)	0.0776 (15)
C(19)	0.5397 (10)	0.0758 (5)	0.0797 (13)
C(20)	0.2313 (13)	0.1992 (7)	−0.2829 (15)
C(21)	0.2869 (15)	0.2468 (11)	−0.3095 (18)
C(22)	0.2756 (21)	0.2981 (11)	−0.2655 (25)
C(23)	0.2090 (18)	0.3029 (8)	−0.2011 (22)
C(24)	0.1550 (12)	0.2566 (7)	−0.1726 (15)
C(25)	−0.0638 (9)	0.1008 (6)	0.1668 (13)
C(26)	−0.0710 (11)	0.1324 (6)	0.2721 (15)
C(27)	−0.0155 (12)	0.1149 (7)	0.3971 (14)
C(28)	0.0404 (12)	0.0676 (7)	0.4124 (13)
C(29)	0.0421 (11)	0.0387 (6)	0.3024 (13)
NP(1)	−0.5307 (20)	0.1028 (10)	−0.3255 (24)
CP(1)	−0.6001 (21)	0.0671 (11)	−0.3076 (23)
CP(2)	−0.6658 (21)	0.0343 (12)	−0.4087 (29)
CP(3)	−0.6380 (19)	0.0409 (10)	−0.5211 (23)
CP(4)	−0.5663 (21)	0.0786 (12)	−0.5375 (24)
CP(5)	−0.5088 (20)	0.1129 (10)	−0.4389 (26)

[a] The standard deviations in parentheses refer to the least significant digit.

For $n = 1$ or 2, $W_{1/2}$ is 90.4 or 45.2 mV, respectively. The values tabulated in Table X are consistent with each uranium redox wave being due to a one-electron reduction. The separation between these two waves measured by differential pulse polarography, ΔE_{DPP}, is also shown in Table X.

For $(UO_2)_2Ni(DBAA)_2$, differential pulse polarographic data were also obtained for the Ni^{2+} reduction wave. A $W_{1/2}$ value of 91 mW was observed. This indicates that the Ni^{2+} reduction is also a one-electron process.

Due to adsorption of products in the cyclic voltammetry and normal pulse polarography experiments a diffusion current could not be measured for the Cu^{2+} reduction in $(UO_2)_2Cu(DBAA)_2$. However, reverse pulse polarography is relatively free from this complication[7] and was used to obtain an accurate value of the diffusion current. The Cu diffusion current is almost exactly half the sum of the diffusion currents for the two uranyl waves. Since a value of $n = 1$ has been determined by differential pulse polarography for each of the uranyl reductions, the number of electrons transferred in the Cu redox process must also be 1.

Discussion

The design and preparation of heteropolynuclear complexes present some interesting synthetic problems. To accomplish a controlled synthesis, one must be able to direct different metal ions, with specificity, to different binding sites within the molecule. In our initial work in this area, we made use of the diamine Schiff-base derivatives of 1,3,5-triketones.[8,9] Such ligands contain two significantly different binding sites (N_2O_2 and O_2O_2), and therefore, one can direct certain metal ions to one site and others to the second site. Generally, this is done by first preparing, isolating, and characterizing the mononuclear complex and then using this complex as a ligand to bind the second metal ion. This approach, of course, depends upon the ligand being asymmetric since it must contain two different binding sites.

Another tack is to develop the required specificity by making use of an unusual coordination geometry of one of the metal ions as a means of orienting the ligands in some optimal manner. The mononuclear UO_2^{2+} 1,3,5-triketonates are an

(6) Parry, E. P.; Osteryoung, R. A. *Anal. Chem.* **1965**, *37*, 1643.
(7) Osteryoung, J.; Kirowa-Eisner, E. *Anal. Chem.* **1980**, *52*, 63.
(8) Tomlonovic, B. K.; Hough, R. L.; Glick, M. D.; Lintvedt, R. L. *J. Am. Chem. Soc.* **1975**, *97*, 2925. Lintvedt, R. L.; Glick, M. D.; Tomlonovic, B. K.; Gavel, D. P. *Inorg. Chem.* **1976**, *15*, 1647, 1654.
(9) Lintvedt, R. L.; Ahmad, N. *Inorg. Chem.* **1982**, *21*, 2356.

Table VII. Bond Distances (Å) and Angles (deg) in the Coordination Spheres of the Metals in $[(UO_2)_2M(DBAA)_2(py)_4]\cdot 2py$

A. Distances

atom 1	atom 2	M: Ni	Co	Fe	Mn
U(1)	M(1)	3.5186 (7)	3.5176 (31)	3.5111 (5)	3.5365 (13)
U(1)	O(1)	2.247 (6)	2.255 (10)	2.249 (7)	2.257 (7)
	O(2)	2.453 (5)	2.471 (9)	2.476 (7)	2.467 (7)
	O(3)[a]	2.465 (5)	2.458 (9)	2.473 (6)	2.473 (6)
	O(4)[a]	2.252 (6)	2.250 (10)	2.265 (7)	2.257 (7)
	O(5)	1.756 (6)	1.756 (9)	1.764 (7)	1.734 (8)
	O(6)	1.763 (6)	1.761 (9)	1.769 (7)	1.743 (8)
	N(1)	2.584 (9)	2.572 (14)	2.564 (11)	2.584 (11)
M(1)	O(2)	2.032 (5)	2.040 (9)	2.053 (7)	2.086 (6)
	O(3)	2.029 (5)	2.046 (8)	2.056 (6)	2.099 (6)
	N(2)	2.175 (6)	2.234 (10)	2.303 (8)	2.377 (9)

B. Angles

atom 1	atom 2	atom 3	M: Ni	Co	Fe	Mn
O(1)	U(1)	O(2)	71.6 (2)	71.3 (3)	70.7 (3)	70.8 (2)
		O(3)[a]	138.8 (2)	139.4 (3)	139.7 (2)	141.0 (2)
		O(4)[a]	148.7 (2)	149.0 (4)	148.8 (3)	148.1 (3)
		O(5)	88.7 (2)	89.3 (4)	89.3 (3)	88.9 (3)
		O(6)	90.5 (3)	91.1 (4)	90.2 (3)	90.7 (3)
		N(1)	73.7 (2)	73.2 (4)	73.5 (3)	72.8 (3)
O(2)	U(1)	O(3)[a]	68.5 (2)	69.2 (3)	70.1 (2)	70.9 (2)
		O(4)[a]	139.5 (2)	139.5 (3)	140.2 (3)	141.0 (2)
		O(5)	95.2 (2)	94.6 (4)	95.2 (3)	93.4 (3)
		O(6)	87.3 (2)	87.6 (4)	86.8 (3)	88.3 (3)
		N(1)	145.1 (2)	144.4 (4)	144.0 (3)	143.5 (3)
O(3)[a]	U(1)	O(4)[a]	72.2 (2)	71.5 (3)	71.2 (2)	70.7 (2)
		O(5)	85.4 (2)	85.1 (4)	85.7 (3)	85.9 (3)
		O(6)	97.1 (2)	96.1 (4)	96.1 (3)	95.7 (3)
		N(1)	146.2 (2)	146.2 (4)	145.8 (3)	145.2 (3)
O(4)[a]	U(1)	O(5)	90.8 (3)	91.2 (4)	90.1 (3)	90.5 (3)
		O(6)	88.4 (3)	87.4 (4)	89.1 (3)	88.8 (3)
		N(1)	75.1 (2)	75.8 (4)	75.4 (3)	75.4 (3)
O(5)	U(1)	O(6)	177.0 (3)	177.8 (5)	177.7 (4)	177.9 (4)
		N(1)	86.7 (3)	87.4 (5)	87.4 (4)	87.0 (4)
O(6)	U(1)	N(1)	90.2 (3)	90.6 (5)	90.3 (4)	90.9 (4)
O(2)	M(1)	O(3)	94.1 (2)	93.6 (3)	92.6 (3)	93.6 (2)
		O(3)[a]	85.9 (2)	86.4 (3)	87.4 (3)	86.4 (2)
		N(2)	88.6 (2)	87.7 (4)	88.7 (3)	88.7 (3)
		N(2)[a]	91.4 (2)	92.3 (4)	91.3 (3)	91.3 (3)
O(3)	M(1)	N(2)	88.2 (2)	88.9 (4)	87.6 (3)	87.3 (3)
		N(2)[a]	91.7 (2)	91.1 (4)	92.4 (3)	92.7 (3)

[a] Atom is located at $\bar{x}, \bar{y}, \bar{z}$.

example since the requirement of a fifth equatorial donor atom forces the two 1,3,5-triketonates to assume a cis-type orienation.[10] In this configuration the UO_2(1,3,5-triketonato)$_2$L complex may be reacted with a second, different metal ion to form the heterobinuclear complex.[9] With this synthetic approach symmetric binucleating ligands may be employed to prepare pure heterobinuclear complexes. In the current study, this same general procedure has been applied to the heterotrinuclear complexes of the symmetric 1,3,5,7-heptanetetrone. Inasmuch as the UO_2^{2+} ions bound to two tetraketonates would most likely be constrained to the terminal coordination sites, the central position is available for a 4-, 5-, or 6-coordinate metal. Although this binuclear UO_2^{2+} complex has not been

Table VIII. Cyclic Voltammetric Data for the Three Waves in $(UO_2)_2Ni(DBAA)_2(py)_4$[a]

scan rate, V/s	$E_{1/2}$, V	ΔE_p, mV	i_{p_a}/i_{p_c}	$i_{p_c}/v^{1/2}$, μA/(mV s^{-1})$^{1/2}$
		First UO_2^{2+} Wave		
0.020	−1.14	80	1.09	5.06
0.050	−1.14	81	1.15	4.84
0.100	−1.14	82	1.11	5.08
0.200	−1.14	90	1.16	4.78
0.500	−1.15	100	1.16	4.69
1.00	−1.15	101	1.13	4.90
2.00	−1.15	112	1.13	4.75
		Second UO_2^{2+} Wave		
0.200	−1.35	74	1.02	5.94
0.050	−1.48	79	1.08	5.77
0.100	−1.35	80	1.07	5.90
0.200	−1.35	87	1.09	5.93
0.500	−1.36	94	1.06	5.84
1.00	−1.36	104	1.10	5.79
2.00	−1.36	124	1.08	6.01
		Ni(II) Wave		
0.020	−1.61	69	1.00	5.27
0.050	−1.61	72	1.07	5.01
0.100	−1.61	71	1.06	4.90
0.200	−1.61	77	1.10	4.78
0.500	−1.61	103	1.16	4.64
1.00	−1.61	101	1.17	4.64
2.00	−1.60	108	1.22	4.16

[a] Saturated solution of $(UO_2)_2Ni(DBAA)_2(py)_4$ in DMF with 0.1 M TEAP at a Pt-disk electrode. All potentials are vs. SSCE.

Table IX. Cyclic Voltammetric Data for the Copper Wave in $(UO_2)_2Cu(DBAA)_2(py)_4$[a]

scan rate, V/s	$E_{1/2}$, V	ΔE_p, mV	i_{p_a}/i_{p_c}	$i_{p_c}/v^{1/2}$, μA/(mV s^{-1})$^{1/2}$
0.020	−0.49	47	0.85	0.575
0.050	−0.49	56	0.92	0.569
0.100	−0.49	65	0.95	0.552
0.500	−0.49	78	1.00	0.553
1.00	−0.49	89	1.02	0.541
5.00	−0.50	130	1.00	0.505

[a] Saturated solution of $(UO_2)_2Cu(DBAA)_2(py)_4$ in DMF with 0.1 M TEAP on a HMDE. All potentials are vs. SSCE.

Table X. Differential Pulse Polarographic Peak Half-Widths and Peak Separations for the Uranyl Reductions in $(UO_2)_2M(DBAA)_2$[a]

M	$W_{1/2}$, mV: first UO_2^{2+} peak	second UO_2^{2+} peak	ΔE_{DPP}, mV
Fe[b]			190
Co	96	94	198
Ni	101	94	220
Cu	106	96	243
Zn	101	96	256

[a] 2.2×10^{-4} M in DMF with 0.100 M TEAP. [b] Due to low solubility only ΔE_{DPP} could be reliably measured.

isolated, it seems a reasonable precursor to the observed products:

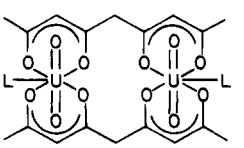

$(UO_2)_2H_2(DBAA)_2(L)_2$

The most surprising aspect of the synthesis of these heterotrinuclear complexes is the ease and specificity with which

(10) Lintvedt, R. L.; Heeg, M. J.; Ahamd, N.; Glick, M. D. *Inorg. Chem.* **1982**, *21*, 2350.
(11) Elder, R. C. *Inorg. Chem.* **1968**, *7*, 2316.
(12) Elder, R. C. *Inorg. Chem.* **1968**, *7*, 1117.
(13) Onuma, S.; Shibata, S. *Bull. Chem. Soc. Jpn.* **1970**, *43*, 2395.

Table XI. Comparison of Average Bond Lengths in $(UO_2)_2M(DBAA)_2(py)_4$ and $M(acac)_2L_2$

	$(UO_2)_2M(DBAA)_2(py)_4$		*trans*-$M(acac)_2L_2$		
M	M-O, Å	M-N, Å	M-O, Å	M-L, Å	ref
Ni	2.029	2.175	2.024	2.112[a]	11
Co	2.046	2.234	2.034	2.187[a]	12
Fe	2.056	2.303			
Mn	2.099	2.377	2.150	2.267[b]	13

[a] L = pyridine. [b] L = H_2O.

they form in the preparative solutions containing 2:2:1 ratios of ligand:UO_2^{2+}:M^{2+}. Indeed attempts were made to prepare 1:1 UO_2^{2+}:M^{2+} and 1:2 UO_2^{2+}:M^{2+} bi- and trinuclear complexes by changing the reaction stoichiometries; however, the only products isolated were the $(UO_2)_2M(DBAA)_2(py)_4$ complexes.

Perhaps the most significant conclusion to draw from the structural results is that the tetraketonate-type ligand has little trouble in binding three metal ions. The flexibility of the carbon backbone is sufficient to accomodate metal–oxygen bond lengths as diverse as the 2.47-Å bond lengths observed for U–O and the 2.03-Å Ni–O bond lengths. As can be seen in Figure 2, this is accomplished by forcing the ends of the ligands out so that the four ketonic oxygens are not linear. The macrocyclic hole that binds the transition-metal ions is apparently very similar in dimensions to the "normal" geometry assumed by the four equatorial oxygens in bis(acetylacetonate) complexes. Bond lengths for the transition-metal ions in $(UO_2)_2M(DBAA)_2(py)_4$ and in $M(acac)_2L_2$ are compared in Table XI. The differences are very small, although there does seem to be a general trend for the transition-metal axial bond lengths in $(UO_2)_2M(DBAA)_2(py)_4$ to be somewhat longer than expected. Since most 1,3-diketonates of Fe(II) are quite air sensitive, no comparable structural data are available for the Fe(II) case. It is, however, curious that $(UO_2)_2Fe(DBAA)_2(py)_4$ was prepared in air and there seems to be no tendency for the Fe(II) to oxidize under these conditions. In fact, for both Fe and Mn this environment appears to yield unusually stable Fe(II) and Mn(II) products.

The UV–visible spectra of these complexes are not very sensitive to changes in the central metal ion, and all consist of two very intense broad bands. As a result of the band centered at about 470 nm, the complexes are extremely intensely colored. The tail of this band gives absorption coefficients of greater than 10^4 at 600 nm. The most logical assignment for the 470-nm band is a L → U(VI) charge-transfer band. The high-energy band at about 260 nm is most reasonably assigned to an intraligand transition. However, the well-developed fine structure has very interesting separation energies. For example, in $(UO_2)_2Ni(DBAA)_2(py)_4$ the four most apparent peaks have λ_{max} of 38 023, 38 911, 39 841 and 40 816 cm^{-1} or separations of 888, 930, and 975 cm^{-1}. Similar values are obtained for the other complexes. This fine structure appears to be due to intraligand pyridine bands.

The cyclic voltammograms of the series all contain two waves separated by about 200 mV that are due to uranium redox with $E_{1/2}$'s of about −1.1 and −1.3 V vs. SSCE. On the basis of the values of i_{p_a}/i_{p_c} and $i_{p_c}/\nu^{1/2}$ for $(UO_2)_2M(DBAA)_2(py)_4$ where M = Ni, Cu, both appear reasonably reversible. The values of ΔE_p are, however, larger than expected and increase with scan rate. Thus, the waves are perhaps best characterized as being quasi-reversible. The peak half-widths of the differential pulse polarograms, $W_{1/2}$, are consistent with each wave being due to the transfer of one electron. The half-width values are somewhat greater than the ideal value of 90.4 mV, which is presumably due to the quasi-reversible nature of the electron transfer. The DPP of Ni^{2+} in $(UO_2)_2Ni(DBAA)_2$ has a half-width of 91 mW, indicative of a one-electron reduction. Additional evidence for the fact that the redox of the uranyl centers involves the transfer of one electron per uranium comes from the CV peak current values. Since the Ni(II) wave is almost certainly due to a one-electron transfer process, its cathodic peak current values, i_{p_c}, are an effective internal standard that can be used to judge the number of electrons transferred in the uranium CV waves. As seen in Table VIII, the i_{p_c} values for three waves at the same scan rates are quite similar. For example, at 0.500 V/s i_{p_c} is 106, 131, and 104 μA, respectively, for the three waves. Thus, on the basis of DPP and CV, the most likely redox process for the two uranium waves is $UO_2^{2+} + e^- \rightleftharpoons UO_2^+$.

Table XII

	CV		DPP	
M	$\Delta E_{1/2}$, mV	K_{con}	ΔE_{DPP}, mV	K_{con}
Fe			190	1.63×10^3
Co	174	8.79×10^2	198	2.23×10^3
Ni	206	3.06×10^3	220	5.26×10^3
Cu	230	7.79×10^3	243	1.29×10^4
Zn	257	2.23×10^4	256	2.14×10^4

Problems with adsorption in the CV of the Cu wave for $(UO_2)_2Cu(DBAA)_2$ on a Pt or Hg electrode make the determination of the number of electrons transferred ambiguous based upon a comparison of UO_2^{2+} and Cu^{2+} cathodic peak currents. For this reason, reverse pulse polarographic experiments were carried out and diffusion currents determined from the results since adsorption problems are often alleviated by RPP.[7] In a typical RPP experiment the diffusion current of the Cu redox is equal to half of the sum of the diffusion currents of the two UO_2^{2+} waves. Since the UO_2^{2+} redox processes have been shown by CV and DPP to be due to one-electrons transfers, the RPP results for the Cu redox prove that it is a one-electron transfer process.

An interesting aspect of the copper redox in $(UO_2)_2Cu(DBAA)_2$ may be seen by comparing its electrochemistry with that of related, but simpler, mononuclear copper complexes of 1,3-diketonates and the Schiff bases of 1,3,5-triketonates.[5] Electrochemical irreversibility is observed for most of the simpler mononuclear complexes while near-reversibility is observed for the copper redox in $(UO_2)_2Cu(DBAA)_2$. This may be due, in part, to the rigid geometry of the planar coordination sphere for Cu in $(UO_2)_2Cu(DBAA)_2$ as compared to the apparent flexibility of the mononuclear complexes. The more rigid coordination geometry may enhance the reversibility of the Cu(II) ⇌ Cu(I) process.

The two one-electron UO_2^{2+} CV waves are separated by about 175–275 mV with the magnitude of the separation being dependent upon the intervening transition-metal ion. From a purely statistical standpoint, if the two UO_2^{2+} centers were noninteracting, one would expect a separation ($E_{1/2}(1) - E_{1/2}(2)$) of only 36 mV at 297 K since the two are in chemically equivalent environments.[14,15] Separations greater than 36 mV are in indication of strengthening interactions between the two redox centers in the sense the larger separations result in greater stability of the mixed-valence product of one-electron reduction. Interactions such as these, resulting in shifts of $E_{1/2}$ values, are generally treated as a conproportionality equilibrium[16] in which $E_{1/2}(1) - E_{1/2}(2) = \Delta E_{1/2} = 0.0591 \log K_{con}$

(14) Flanagan, J. B.; Margel, S.; Bard, A. J.; Anson, F. C. *J. Am. Chem. Soc.* **1978**, *100*, 4248.
(15) Ammar, F.; Saviant, J. M. *J. Electroanal. Chem. Interfacial Electrochem.* **1973**, *47*, 115, 215.
(16) Gagné, R. R.; Koval, C. A.; Smith, T. J.; Cimolino, M. C. *J. Am. Chem. Soc.* **1979**, *101*, 4571.
(17) De Muelenaer, J.; Tompa, H. *Acta Crystallogr.* **1965**, *19*, 1014–1018.
(18) Templeton, L. K.; Templeton, D. H. American Crystallographic Assoication Meeting, Storrs, CT, 1973, Abstract E-10.

where

$$(Ox,Ox) + (Red,Red) \overset{K_{con}}{\rightleftharpoons} 2(Ox,Red)$$

The K_{con} values determined for the series from CV values of $\Delta E_{1/2}$ and from the DPP values of the peak separations (Table X) are tabulated in Table XII. Reliable CV values for M = Fe, Mn or DPP values for M = Mn could not be obtained due to distortions brought about by small separations. The ease of measuring peak separations by DPP probably make the K_{con} values determined by DPP more dependable than those obtained from CV. However, in most cases the differences are not very great, generally within a factor of about 2. The results, in either case, clearly demonstrate that the stability of the mixed U(VI), U(V) species is dependent upon the intervening divalent metal ion and increases in a periodic manner from M = Fe to M = Zn. The structural results do not give any obvious clues to the origin of this periodicity. Except for the usual variation in M-O bond lengths for M = Ni, Co, Fe, Mn, the structures do not exhibit obvious periodic difference especially in the plane of the tetraketonates. Unfortunately, we have not succeeded in preparing and characterizing the binuclear UO_2^{2+} complex with the central position vacant. Similar studies on it could presumably furnish direct information on the importance of an intervening metal ion.

Acknowledgment. This work was supported by the National Science Foundation (Grant No. CHE 83-00251).

Registry No. $[(UO_2)_2Mn(DBAA)_2(py)_4]\cdot 2py$, 91238-59-4; $[(UO_2)_2Fe(DBAA)_2(py)_4]\cdot 2py$, 91238-61-8; $[(UO_2)_2Co(DBAA)_2(py)_4]\cdot 2py$, 91238-63-0; $[(UO_2)_2Ni(DBAA)_2(py)_4]\cdot 2py$, 81205-64-3; $[(UO_2)_2Cu(DBAA)_2(py)_4]$, 91238-64-1; $[(UO_2)_2Zn(DBAA)_2(py)_4]$, 91238-65-2.

Supplementary Material Available: Listings of bond distances and angles, hydrogen atom parameters, thermal parameters, and observed and calculated structure factors (×10) (86 pages). Ordering information is given on any current masthead page.

(19) Cromer, D. T.; Waber, J. T. In "Internatinal Tables for X-ray Crystallography"; Ibers, J. A., Hamilton, W. C., Eds.; Kynoch Press: Birmingham, England, 1974,; Vol. IV, pp 71-147.
(20) Cromer, D. T.; Waber, J. T. In ref 19, pp 148-151.
(21) Stewart, R. F.; Davidson, E. R.; Simpson, W. T. *J. Chem. Phys.* **1965**, *42*, 3175-3187.

Contribution from the Departments of Chemistry, North Carolina State University, Raleigh, North Carolina 27650, and University of Georgia, Athens, Georgia 30602

Multiple Luminescence from Borohydridobis(triphenylphosphine)copper(I)

DONALD P. SEGERS,† M. KEITH DEARMOND,*† PAUL A. GRUTSCH,‡ and CHARLES KUTAL‡

Received December 28, 1983

Low-temperature (77 K) luminescence spectra and lifetimes have been measured for the $Cu(PPh_3)_2BH_4$ (PPh_3 is triphenylphosphine) and Cu(prophos)BH_4 (prophos is 1,3-bis(diphenylphosphino)propane) complexes. $Cu(PPh_3)_2BH_4$ exhibits multiple emission from $^3\Pi\Pi^*$ and $^3(\sigma\text{-}a_\pi)$ excited states in appropriate solvents, while Cu(prophos)BH_4 shows only a single $^3(\sigma\text{-}a_\pi)$ emission in most of the solvents chosen for this study. The electronic transition associated with the $\sigma\text{-}a_\pi$ assignment is analogous to the $l\text{-}a_\pi$ transition for the free phosphine ligand. These unique emission results are discussed in terms of intramolecular and intermolecular (solvent-solute) effects.

Introduction

The occurrence of multiple-state emission,[1] specifically dual phosphorescence, for transition-metal complexes has two origins that may not be mutually exclusive: (1) spatially isolated (single (chelate)-ring and (2) distinct-orbital emission. The spatially isolated emission is most directly illustrated by the dual phosphorescence exhibited by the $[Rh(bpy)_2phen]^{3+}$ and $[Rh(phen)_2bpy]^{3+}$ complexes.[2] A more subtle but related single-ring emission has been characterized for the $[Ru(bpy)_3]^{2+}$ complex ion with use of excited-state resonance Raman[3] and photoselection[4] spectroscopy. The multiple emissions described here each have the same orbital origin, $\Pi\Pi^*$ for the Rh(III) complexes and $d\Pi^*$ for $[Ru(bpy)_3]^{2+}$ (and a number of its derivatives), and, at present, has only been identified for nominally d^6 complexes. In contrast, the second type of multiple emission, distinct orbital, has been observed not only for d^6 complexes[5,6] but also for d^8 Re(I) complexes[7] and most recently for d^{10} Cu(I) complexes.[8] Here the two phosphorescence emission bands differ in their orbital origin with such combinations as $dd^*\text{-}d\Pi^*$,[5] $dd^*\text{-}\Pi d^*$,[6] and $d\Pi^*\text{-}\Pi\Pi^*$[8] having been observed. In these latter cases emission spectra and lifetimes can be used to identify the multiple-state emission with appropriate extreme precaution taken to ensure purity and identity of the emitting material.

At the inception of this work, the only multiple-state Cu(I) emitters were those reported by McMillin and co-workers[8] for $[Cu(PPh_3)_2L]^+$ (PPh_3 is triphenylphosphine) complexes where L is a diimine ligand, e.g., 1,10-phenanthroline. These emissions were assigned as occurring from intraligand ($\Pi\Pi^*$) and metal-to-ligand charge-transfer ($d\Pi^*$) excited states, both of which were associated with the diimine ligand. Recently, Kutal and co-workers determined[9] that Cu(I) complexes such

† North Carolina State University.
‡ University of Georgia.

(1) M. K. DeArmond and C. M. Carlin, *Coord. Chem. Rev.*, **36**, 325 (1981).
(2) W. Halper and M. K. DeArmond, *J. Lumin.*, **5**, 225 (1972).
(3) P. G. Bradley, N. Kress, B. A. Hornberger, R. F. Dallinger, and W. H. Woodruff, *J. Am. Chem. Soc.*, **103**, 7441 (1981).
(4) C. M. Carlin and M. K. DeArmond, *Chem. Phys. Lett.*, **89**, 297 (1982).
(5) (a) R. J. Watts, T. P. White, and B. G. Griffith, *J. Am. Chem. Soc.*, **97**, 6914 (1975); (b) R. J. Watts and D. Missimer, *ibid.*, **100**, 5350 (1978).
(6) J. T. Merrill and M. K. DeArmond, *J. Am. Chem. Soc.*, **101**, 2045 (1979).
(7) (a) P. J. Giordano, S. M. Fredericks, M. S. Wrighton, and D. L. Morse, *J. Am. Chem. Soc.*, **100**, 2257 (1978); (b) S. M. Fredericks, J. C. Luong, and M. S. Wrighton, *ibid.*, **101**, 7415 (1979).
(8) (a) M. T. Buckner, T. G. Matthews, F. E. Lytle, and D. R. McMillin, *J. Am. Chem. Soc.*, **101**, 5846 (1979); (b) R. A. Rader, D. R. McMillin, M. T. Buckner, T. G. Matthews, D. J. Casadonte, R. K. Lengel, S. B. Whittaker, L. M. Darmon, and F. E. Lytle, *ibid.*, **103**, 5906 (1981).
(9) (a) P. A. Grutsch and C. Kutal, *J. Am. Chem. Soc.*, **99**, 6460 (1977); (b) P. A. Grutsch and C. Kutal, *ibid.*, **101**, 4228 (1979); (c) S. W. Orchard and C. Kutal, *Inorg. Chim. Acta*, **64**, 195 (1982).

0020-1669/84/1323-2874$01.50/0